ELSEVIER

Journal of Alloys and Compounds 323–324 (2001) 239–244

Journal of ALLOYS AND COMPOUNDS

www.elsevier.com/locate/jallcom

# Laser-induced internal cooling of $Yb^{3+}$-doped fluoride-based glasses

J. Fernández[a,b,*], A. Mendioroz[a], A.J. García[a], R. Balda[a,b], J.L. Adam[c]

[a]*Departamento de Física Aplicada I, E.T.S.I.I. y Telecom., Alda. Urquijo s/n, 48013 Bilbao, Spain*
[b]*Centro Mixto CSIC-UPV/EHU, E.T.S.I.I. y Telecom., Alda. Urquijo s/n, 48013 Bilbao, Spain*
[c]*Laboratoire de Verres et Céramiques, Université de Rennes I, UMR-CNRS 6512, Campus de Beaulieu, 35042 Rennes Cedex, France*

**Abstract**

Laser-induced internal cooling between room temperature and 77 K in a new fluorochloride glass (CNBZn) and a fluoride glass (BIG) doped with 1 mol% of $YbF_3$ has been demonstrated by using collinear photothermal deflection and conventional laser excitation spectroscopies under high photon irradiances. The cooling efficiency for CNBZn glass which is ~2.0% relative to the absorbed laser power at 1010 nm and 300 K falls about 20% at 77 K. The cooling efficiency for BIG glass was only ~0.6% at room temperature. The experimental results are in good agreement with the predictions of a model based on the hypothesis of a second order process for the cooling mechanism. 

*Keywords:* Amorphous materials; Electron–phonon interactions; Optical properties; Phonons; Luminescence

## 1. Introduction

At the beginning of this century, Pringsheim [1] suggested the possibility of cooling an object through its interaction with radiation. Twenty years later, Kastler [2] proposed that cooling could result from the anti-Stokes emission of rare-earth doped crystals, but the attempts to achieve cooling in solids by means of this effect resulted in reduced heating rates [3] for a long time. In 1995, the first experimental evidence of laser cooling in a solid was presented [4], in particular, for an $Yb^{3+}$-doped fluorozirconate glass. From then on, several works have been published regarding topics as the composition requirements of the matrices to achieve cooling [5–7] or the temperature drop attainable in fiber configuration [8–10]. Moreover, cooling has also been observed in liquids [11] and semiconductors [12].

Among the potential applications of anti-Stokes laser cooling of solids, two main fields seem to attract the interest on this effect: cryocoolers for aerospatial applications and high power solid state lasers in which no excess heat is generated.

The low temperature cooling efficiency of glasses has been investigated in two fluorozirconate glasses and a phosphate glass [6] by measuring the absorption and emission spectra of the samples at different temperatures and evaluating the cooling efficiencies when pumping the sample at a wavelength which corresponds to an absorption coefficient of $10^{-3}$ $cm^{-1}$. The results reveal the BIGaZYbTZr ($BaF_2$–$InF_3$–$GaF_3$–$ZnF_2$–$ThF_4$–$ZrF_4$) glass as the best candidate, showing an efficiency of twice that of ZBLAN glass at 50 K. Theoretical studies on the capability of rare-earth doped glasses as low temperature coolers [13] point out to an actual ability of the studied glass ($Yb^{3+}$-doped ZBLAN glass) to work as a cryocooler. On the other hand, the technical problems such as laser losses, luminescence efficiency, evacuation of luminescent light, adequate path lengths, high optical quality of components, suitable laser sources etc. seem to be surmountable.

Regarding the second field of interest, Bowman [14] proposed to use radiation cooling by anti-Stokes fluorescence within the laser medium to balance the heat generated by the Stokes shifted stimulated emission (radiation balanced lasers). This could arise in very high power lasers in which limitations in beam quality and average power could be overcome. The studies carried out to evaluate ytterbium-doped laser materials for their utility in radiation balanced laser systems [15] predict that $Yb^{3+}$-doped $KY(WO_4)_2$ and $KGd(WO_4)_2$ crystals will show the high-

*Corresponding author. Tel.: +34-94-601-4044; fax: +34-94-601-4178.

*E-mail address:* wupferoj@bi.ehu.es (J. Fernández).

0925-8388/01/$ – see front matter 
PII: S0925-8388(01)01051-9

est performance in this kind of systems. In these studies, fluorescence optical cooling in $KGd(WO_4)_2$ crystal has been reported for the first time, which opens a very encouraging outlook for radiation balanced lasers.

In this work, we present experimental evidences of laser cooling in two bulk $Yb^{3+}$-doped fluorochloride and fluoride glasses. These results have been obtained by using two different techniques: collinear photothermal deflection spectroscopy and conventional laser excitation spectroscopy performed under the same high photon irradiances. The photothermal measurements give similar results to those found in fluorozirconate glass and show similar cooling efficiencies [6]. However, the spectroscopic results clearly reveal that the cooling range is restricted to a narrow spectral region which depends on the phonon density of states of the material. Moreover, the thermal dependence of the additional fluorescence which appears in the excitation spectra as a consequence of cooling, makes clear that the cooling efficiency is a function of temperature.

## 2. Experimental

Two samples of CNBZn glass ($CdF_2$–$CdCl_2$–NaF–$BaF_2$–$BaCl_2$–$ZnF_2$) and BIG ($BaF_2$–$InF_3$–$GaF_3$–$ZnF_2$–$LuF_3$–$GdF_3$) glass doped with 1 mol% of $YbF_3$ were investigated. The samples of dimensions 2×8×10 mm were suspended from a silk wire cross inside a cryostat evacuated to ~$10^{-2}$ mbar to improve thermal isolation. Fig. 1 shows a block diagram of the experimental set-up. The beam of a tunable ($\lambda$=905–1090 nm) CW titanium–sapphire ring laser (8 GHz bandwidth) which entered the sample perpendicularly to the center of the 2×8 mm face was modulated at 1.24 Hz by means of a mechanical chopper. A fraction of the incident power was utilized for signal normalization. A copropagating helium–neon probe laser beam ($\lambda$=632.8 nm) was co-aligned with the pump beam through a dichroic element. Both pump and probe copropagating beams were focused into the middle of the sample with diameters of ~100 and ~60 μm, respectively. After leaving the sample, the beams passed through a second identical lens separated from the first one by a distance twice the focal length (5 cm) to avoid high divergence of the emerging beams. A second dichroic beam splitter deviated the pumping beam to a pyroelectric detector which measured the transmitted pumping power. Before reaching a quadrant position detector the probe beam passed through an interference filter to eliminate residual pumping radiation. The excitation spectra were measured with the same configuration by collecting the fluorescence at a right-angle from the focused area of the pumping beam by means of a collimating lens, and focusing it with a second lens at the 100-μm entrance slit of a 0.22-m monochromator provided with an extended infrared photomultiplier. Lock-in detection was used in both experiments. Thermal deflection waveforms were detected by using a digital scope.

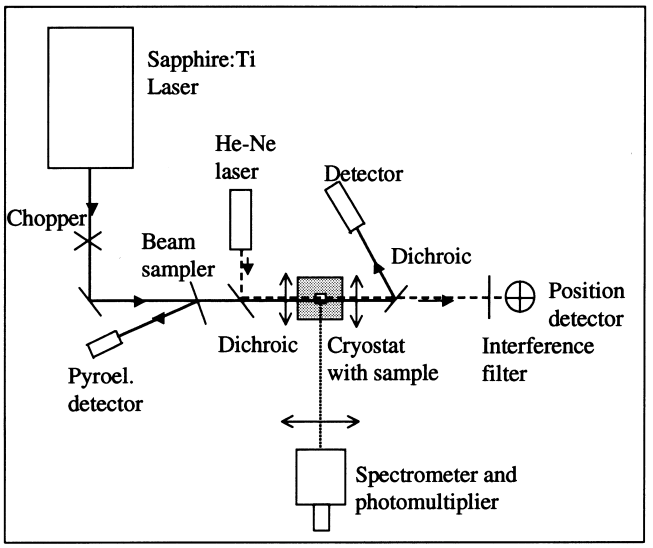


Fig. 1. Block diagram of the experimental set-up used in the photothermal deflection, absorption, and excitation measurements.

## 3. Results

### 3.1. Photothermal quantum efficiency measurements

The evaluation of the quantum efficiency (QE) has been carried out by considering a simplified model of the $Yb^{3+}$ ions as a two level system (Fig. 2). We shall consider a typical process in which a photon of energy $\hbar\omega_L$ from the incident beam of intensity $I_0$ modulated at a frequency of $\omega_m$ is absorbed by an electron that goes up to the excited state. The relaxation to the ground state can take place through radiative or non-radiative processes with probabilities $W_R$ and $W_{NR}$, respectively, at a mean energy of $\hbar\omega_0$. The energy difference between the incident and fluorescent photons is exchanged as heat with the host.

In this model, the heat the sample exchanges per unit time and unit volume in a typical heating process is:

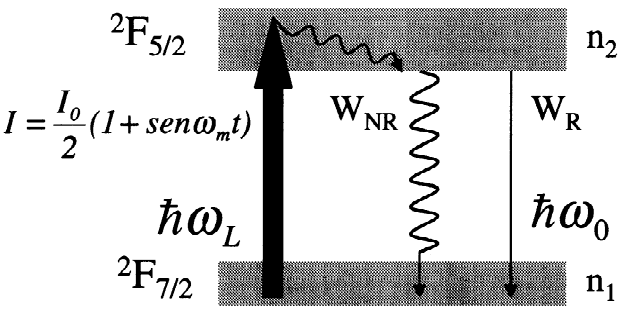


Fig. 2. Two level scheme of the $Yb^{3+}$ ions in a typical heating process.

$$H = n_2[W_{NR}\hbar\omega_L + W_R\hbar(\omega_L - \omega_0)] \quad (1)$$

where $n_2$ is the population density of the excited state.

The excited state population is governed by the incident beam modulation frequency $\omega_m$ and the lifetime of the level, $\tau$:

$$\frac{dn_2}{dt} = n_1 \frac{\sigma I}{\hbar\omega_L} - \frac{n_2}{\tau} \quad (2)$$

where $\sigma$ is the absorption cross section and $n_1$ is the population of the ground state.

If we solve this equation and enter the result in Eq. (1), we find the following result [16]:

$$H(\omega) = \frac{I_0}{2} n_1 \sigma\left(1 - \eta\frac{\omega_0}{\omega_L}\right) \cos\Phi \,\mathrm{sen}(\omega_m t + \Phi) \quad (3)$$

where $\Phi = \tan^{-1}(\omega_m\tau)$ is the phase relative to the incident modulation beam.

In the case of low modulation frequency, $\tau\omega_m \ll 1$ the heat the sample exchanges per unit time and unit volume takes a very simple form:

$$H = n_1\sigma I_0\left[1 - \eta\frac{\omega_0}{\omega_L}\right] \quad (4)$$

where $\eta$ is the fluorescence QE of the excited state, that is defined as the ratio of the radiative relaxation probability to the total relaxation probability:

$$\eta = \frac{W_R}{W_R + W_{NR}} = W_R\tau$$

In this collinear configuration, the amplitude of the angular deviation of the probe beam is always proportional to the amount of heat the sample exchanges, whichever its optical or thermal properties are [17]. This allows to relate the amplitude of the deflection at each wavelength to the typical relaxation parameters of the $Yb^{3+}$ ions after the absorption of the pumping radiation, in particular to the QE of the $^2F_{5/2} \rightarrow {}^2F_{7/2}$ transition, giving thus:

$$\frac{PDS}{n_1\sigma I_0} = C\left[1 - \eta\frac{\omega_0}{\omega_L}\right] = C\left[1 - \eta\frac{\lambda_L}{\lambda_0}\right] \quad (5)$$

As can be seen the normalized photothermal deflection signal divided by the absorption of the sample has a linear dependence with the pumping wavelength. From the slope and intercept of this straight line, and by using the value of the mean fluorescence wavelength (at which the zero deflection signal occurs), the QE $\eta$ can be obtained.

The room temperature photothermal deflection signal waveforms of the CNBZn and BIG glasses were recorded in the scope for different pumping wavelengths. Fig. 3 shows the deflection signal waveforms in the case of BIG. The zero signal occurs around 985 nm. The lock-in phase and amplitude of the photothermal deflection, normalized by the absorption, for the CNBZn sample, are displayed in Fig. 4 as a function of the pumping wavelength. As predicted by theory [18], a neat change of about 180°C can be observed during the transition from the heating to the cooling region, at around 988 nm (Fig. 4a). The QE in the heating region as measured from the photothermal amplitude and absorption [16,17] was $0.996 \pm 3.23 \times 10^{-6}$ and the one at the beginning of the cooling region (from 988 to 1010 nm), $1.016 \pm 1.54 \times 10^{-5}$. Therefore, the cooling efficiency estimated by using the QE measurements is about 2.0%. In the case of BIG glass, the estimated cooling efficiency (983–1010 nm region) was only 0.6%. It is worthy to notice the nonlinear dependence of the photothermal deflection amplitude with the pumping wavelength in the whole cooling region. This behavior impedes photothermal QE measurements at wavelengths longer than 1010 nm. As we shall see in the next section, this broad peak formed by the photothermal deflection approximately resembles the one observed for the excess of luminescence associated with cooling, thus confirming the nonlinear behavior of this process.

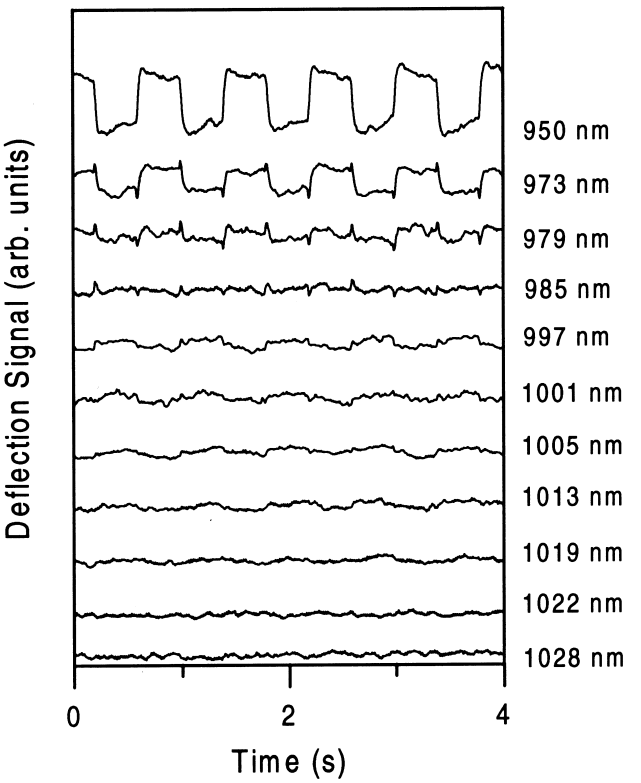


Fig. 3. Photothermal deflection signal waveforms obtained for the BIG sample at room temperature.

### 3.2. Excitation spectra

To further investigate the origin of the observed cooling, we performed excitation measurements in both samples at

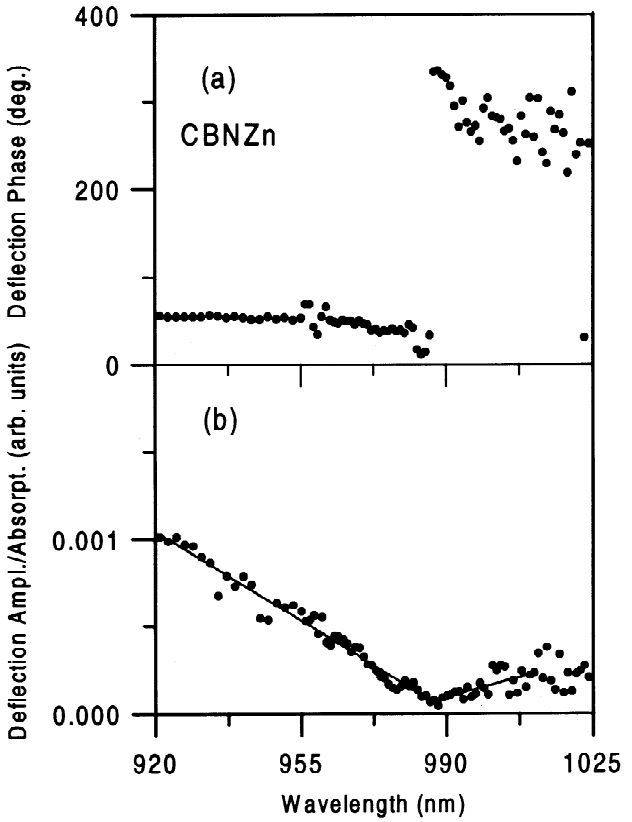


Fig. 4. (a) Phase of the photothermal deflection signal and (b) photothermal deflection amplitude (normalized by the incident laser power) divided by the absorption of the CNBZn glass sample at each wavelength, measured with the lock-in amplifier at room temperature.

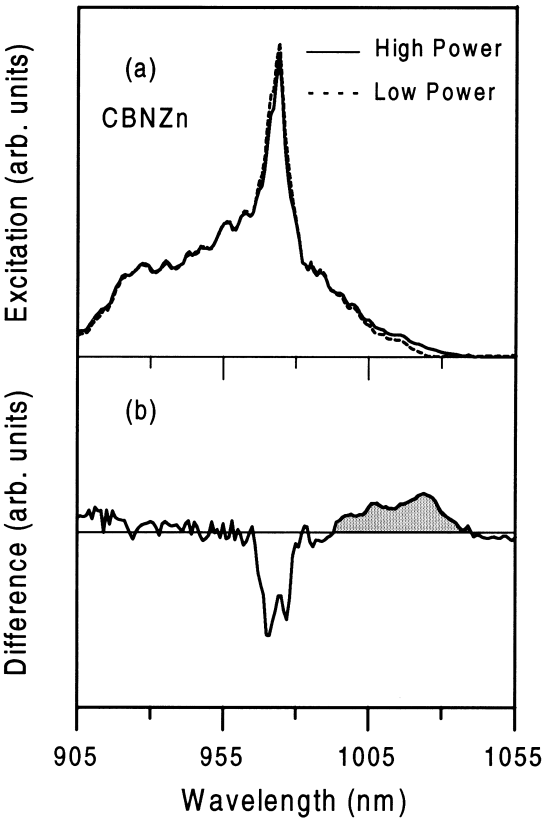


Fig. 5. (a) High power (solid line) and low power (dashed line) excitation spectra recorded at 1040 nm and 225 K in CNBZn glass. (b) Difference between the high and low power spectra. The shaded area corresponds to the cooling luminescence.

different pumping photon irradiances and temperatures by keeping the system in the same conditions. As an example, Fig. 5a shows the excitation spectra measured at 225 K for the CNBZn glass collecting the luminescence at 1040 nm (at the end of the cooling zone) and at two different pumping irradiances, 880 and 150 mW. Fig. 5b displays the normalized difference of both spectra. As we can see, except for the zone around the main absorption peak where an accurate difference is difficult to obtain (probably due to some saturation in the spectrum taken at high irradiances), the difference mainly consists of a broad peak (shaded region in Fig. 5b) which covers the spectral range where cooling occurs. This new peak must correspond to the excess of fluorescence produced as a consequence of the cooling process which allows for an additional population of the excited state in this region. This means that at high photon irradiances, other than first order processes are playing a principal role in this spectral range.

The dependence with pumping power of the broad peak integrated intensity, which corresponds to the cooling luminescence, is close to linearity whereas it shows a nonlinear temperature dependence. Fig. 6a and b show the integrated intensity of the cooling fluorescence peak as a function of temperature for both glasses.

## 4. Discussion

The experimental integrated intensities of the cooling fluorescence band have been compared with the predictions of a theoretical model that proposes a cooling mechanism in which an $Yb^{3+}$ ion in its ground state absorbs an incident photon and a phonon of the glass matrix and goes up to the excited state [19].

The model predicts the probability of such a second order process, given by:

$$I(T) \approx \int_0^{\omega_D} \frac{x}{\omega_0 - x} \exp\left[ -\left(\frac{x-\bar{\omega}}{\Delta\omega}\right)^2 \right] \frac{1}{\exp\left(\frac{x}{k_B T}\right) - 1} \mathrm{d}x \tag{6}$$

where $\omega_D$ is the Debye frequency, $x$ is the frequency difference between the mean fluorescence photon and the incident photon, $\bar{\omega}$ is the frequency corresponding to the centre of a gaussian phonon density of states of the material, $\Delta\omega$ is its width, $k_B$ is the Boltzmann constant, and $T$ is the absolute temperature. In order to compare the experimental results with the numerical evaluation of Eq.

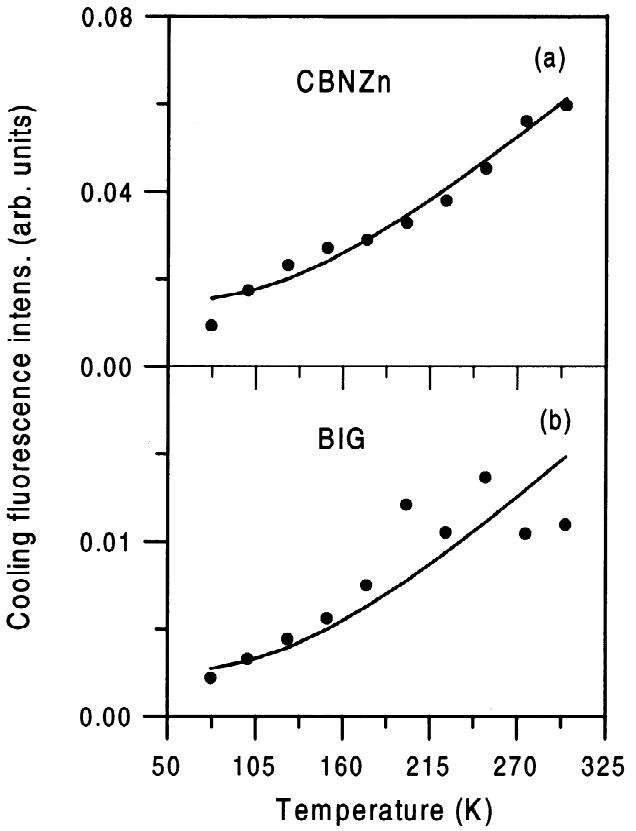


Fig. 6. Experimental cooling fluorescence integrated intensities as a function of temperature (dots) and fitting to Eq. (7) (solid line) for CNBZn glass (a) and BIG glass (b).

(6), the effect of inhomogeneous broadening is included by adding a constant background independent on temperature:

$$i(T) = a + bI(T) \quad (7)$$

The continuous line appearing in Fig. 6a and b is the fitting with the theoretical model given by Eq. (7). The only parameters used in this fitting are the constants in Eq. (7) accounting for the inhomogeneous broadening.

As we can see, the agreement between experimental results and theory is very good supporting the model hypothesis about the kind of processes involved. Moreover, if we compare the relative integrated intensities at different temperatures we can have a real picture about the temperature dependence of the cooling efficiency of the material. Our experimental results in these glasses show it is possible to cool an internal volume from room temperature down to 77 K but with a penalty of about a 20% in the cooling efficiency (cooling efficiency is defined as the ratio of the integrated cooling fluorescence peak to the integrated intensity of the high power excitation spectrum without the cooling peak contribution).

It is worthy to mention the quite good agreement between the room temperature cooling efficiencies obtained by using photothermal QE measurements and the ones obtained by measuring the fluorescence excess from the excitation spectra. In the former case efficiencies of 2 and 0.6%, respectively, were found for CNBZn and BIG glasses, whereas in the second case values of 3 and 1%, respectively, were obtained for the same samples.

## 5. Summary

Laser cooling in a fluoride and a fluorochloride glass has been demonstrated at room temperature using photothermal deflection spectroscopy and excitation and absorption spectroscopies.

The cooling efficiency of both glasses has been evaluated at room temperature by using two different experimental techniques. The results from both techniques are in good agreement for both glasses. The fluorochloride glass shows a slightly higher efficiency.

The cooling efficiency has been evaluated in both glasses from 77 K to room temperature from the high and low power excitation spectra. The efficiency at 77 K falls to about 20% of its value at room temperature.

The experimental results are in good agreement with the predictions of a theoretical model based on the hypothesis of a second order process for the cooling mechanism.

## Acknowledgements

This work has been supported by the Basque Country University (G21/98), Spanish Government CICYT (Ref. MAT97-1009), (DGICYT Ref. PB95-0512), (HF-1998-0154), and Basque Country Government (PI97/99).

## References

[1] P. Pringsheim, Z. Phys. 57 (1929) 739.
[2] A. Kastler, J. Phys. Radium 11 (1950) 255.
[3] T. Kushida, J. Geusic, Phys. Rev. Lett. 21 (1968) 1172.
[4] R.I. Epstein, M.I. Buchwald, B.C. Edwards, T.R. Gosnell, C.E. Mungan, Nature 377 (1995) 500.
[5] J. Fajardo, G.H. Sigel Jr., B.C. Edwards, R.I. Epstein, T.R. Gosnell, C.E. Mungan, J. Non-Cryst. Solids 213 (1997) 65.
[6] G. Lei, J.E. Anderson, M.I. Buchwald, B.C. Edwards, R.I. Epstein, M.T. Murtagh, G.H. Siegel Jr., IEEE J. Quantum Electron. 34 (1998) 1839.
[7] M.T. Murtagh, G.H. Siegel Jr., J. Fajardo, B.C. Edwards, R.I. Epstein, J. Non-Cryst. Solids 257 (1999) 207.
[8] C.E. Mungan, M.I. Buchwald, B.C. Edwards, R.I. Epstein, T.R. Gosnell, Phys. Rev. Lett. 78 (1997) 1030.
[9] X. Luo, M.D. Eisaman, T.R. Gosnell, Opt. Lett. 23 (1998) 639.
[10] T.R. Gosnell, Opt. Lett. 24 (1999) 1041.
[11] J.L. Clark, G. Rumbles, Phys. Rev. Lett. 76 (1996) 2037.
[12] E. Finkeiβen, M. Potemski, P. Wyder, Appl. Phys. Lett. 75 (1999) 1258.
[13] G. Lamouche, P. Lavallard, R. Suris, R. Grousson, J. Appl. Phys. 84 (1998) 509.
[14] S.R. Bowman, IEEE J. Quantum Electron. 35 (1999) 115.

[15] S.R. Bowman, C.E. Mungan, in: Advanced Solid State Lasers, OSA Trends in Optics and Photonics Series, 1999, p. 156.
[16] J. Etxebarria, J. Fernández, J. Phys. C 16 (1983) 3803.
[17] A. Salazar, A. Sánchez-Lavega, J. Fernández, J. Appl. Phys. 74 (1993) 1539.
[18] W.B. Jackson, N.M. Amer, A.C. Boccara, D. Fournier, Appl. Opt. 20 (1981) 1333.
[19] J. Fernández, A. Mendioroz, A.J. García, R. Balda, J.L. Adam, Opt. Mater. 16 (2001) 173.